GAS Journal of Engineering and Technology (GASJET)

Volume 2 | Issue 12, 2025 Homepage: https://gaspublishers.com/gasjet-home/ ISSN: 3048-5800

DC Current Offset Compensation Method for Grid-Connected Inverter

Song IL Rim, Sunghyok Kim and Songchol Hyon

Faculty of Electrical Engineering, Kim Chaek University of Technology, Pyongyang, Democratic People's Republic of Korea

Received: *10.11.2025* | ***Accepted:*** *22.11.2025* | ***Published:*** *12.12.2025*

***Corresponding Author:** Songchol Hyon

DOI: *10.5281/zenodo.17914276*

Abstract **Original Research Article**

Grid-connected inverters without isolated transformers are widely used because of their high efficiency, small size and mass, however this converter has a negative effect on the grid due to the DC current offset occurred at the inverter output. One of the major problems to overcome in the control of grid-connected converters is the DC offset existed in measurement. Also, the current offset in one phase results in the one of the other phases due to the correlation among three phase currents unlike single-phase and accordingly, the current offset of each phase cannot be removed by only measuring. In this paper, a method for removing the DC current offset by using both observer and compensation method is proposed for three-phase grid-connected inverter. By using the observer, the current offset is obtained by filtering of the deference between the grid current and the output reference current extracted from the grid voltage and switching state. Also, without the conventional DC offset PI controller, the DC current offset directly inputs as the DC offset reference of the current controller in the rotating reference frame. The proposed DC offset compensation method is validated on a 10 kW grid-connected converter using MATLAB.

Keywords: Current offset compensation, DC current offset, three-phase grid-connected inverter, and rotating reference frame control.

I. INTRODUCTION

Transformer less grid connected inverters are widely used because of their high efficiency, small size and mass. However, the dc current offset generated at the inverter output causes negative problems like the dc magnetization in the grid transformer [1]-[3]. The dc current injected by the transformerless PV inverter increases the no-load dc component current of the distribution transformers, saturates the transformers, and severely distorts the output voltage waveform [15, 22].

Several methods have been proposed to eliminate the dc current offset. These methods mainly divided into hardware and software methods.

The hardware methods include the capacitor-based method, the current transformer-based method, the DC current detection method, the converter output voltage detection circuit method and the new converter type selection. Capacitor elimination is a method to remove the dc component from the AC current by connecting a large capacitor in series to the output stage [4]. However, this method requires the use of a large capacitor, which results in a large

volume, high cost and additional losses. Current transformer methods are the method that eliminate DC current offset by adding an additional current transformer to the output [5, 21]. These methods require additional circuits and increase the volume and cost due to the need to install additional circuits that can flow with large currents in case of increased converter power. To reduce the size and increase the measurement accuracy, a method using the additional winding and customized current sensor has been proposed, but additional windings should be included to form a circuit and measures should be taken to prevent saturation and phase difference of the current transformer [23]. The DC current detection method should use a high-accuracy sensor and is highly dependent on the characteristics of the Hall current sensor. To improve the performance, an automatic calibration method is proposed. However, the calibration process requires double the sampling rate and the method is only effective for limited topologies and dc sources [6, 20]. The method with the converter output voltage detection circuit should use an additional voltage sensing circuit [7]-[9]. These methods are based on voltage feedback. However, these methods should use a high-accuracy voltage sensor [16]-[18]. There is also a way to choose a new converter type, where additional switching elements should be added [10].

The software methods include the observer-based method, the virtual capacitor-based method and the intelligent control method. A method using an observer to calculate the current offset has been proposed, but this method is only applicable to single-phase grid-connected converters [11]. There are also methods using virtual capacitors, where the dynamic response of the closed-loop system is affected by the virtual capacitors [12, 13]. Intelligent control method is proposed in [19], this method depends on the accuracy of the current measurement.

The sensed current signal has a current offset in each phase, making it difficult to discern which phase has a current offset. To accurately identify the current offset, the grid current must be calculated accurately.

In addition, the three-phase grid current flows in relation to other phases, so that the current offset generated in one phase correlates with other phases, causing current offset in the phases. On the other hand, current offset cannot be compensated by directly removing the current bias from the current measurement.

Hence, we propose a method to calculate the grid current based on the output voltage of the converter, grid voltage and filter parameters, and a method to calculate the current offset using the measured grid current. In addition, a method to compensate the current bias in the rotating reference frame is proposed. In this paper, the method to compensate the current offset based on the current observer without additional circuit or structural modifications to eliminate the current offset is proposed.

This paper is organized as follows: In Section 1, the current offset reduction method for grid-connected converter is introduced. In Section 2, we describe the background in which the paper is presented. In Section 3, the proposed current offset compensation method is described. In Section 4, the characteristic analysis of the proposed current offset compensation method is presented.

II. Background

Fig. 1 shows the original scheme diagram of the grid-connected inverter. The inverter connected to the DC bus of u_{dc} generates the voltage u_{inv_i} at the output. The voltage is applied to the grid of u_{g_i} through a filter, where r_i and L_i are the internal resistance and the inductance of the filter, respectively. The subscript i is a, b, c.

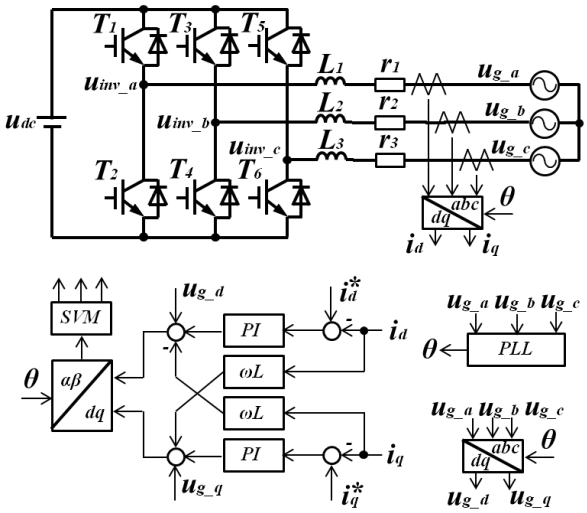

Fig. 1. Original scheme diagram of three-phase grid-connected inverter.

In the grid-connected inverter, the phase of the grid voltage is measured by a phase locked loop (PLL). Then the *dq* components of the grid voltage and inverter output current are obtained by Clarke and Park transformation.

The active and reactive powers are regulated through the output current of the inverter. The reference output current of the current controller is then set by the droop controller or the virtual synchronous generator. As the current controllers, the proportional resonant (PR) controller in the stationary reference frame and the proportional integrator (PI) controllers in the rotating reference frame can be used [14]. The PR controller has good control performance, but the current tracking performance is poor in the frequency-varying system, whereas the PI controllers are stable regardless of the frequency variation. However, in a rotating reference frame, the DC offset current occurring during current detection also impacts on the *dq* components of the output current, resulting in asymmetry of the three-phase current and the DC current injection.

The current detection error includes the errors by the sensor, the sensor circuit and the analog-to-digital converter [8].

If the current of one phase is offset, the *dq* output currents oscillate as the supply frequency. The output currents are expressed in the rotating reference frame as follows:

$$\begin{pmatrix} i_d \\ i_q \\ i_0 \end{pmatrix} = \frac{2}{3} \begin{pmatrix} \sin\omega t & \sin(\omega t - \frac{2\pi}{3}) & \sin(\omega t + \frac{2\pi}{3}) \\ \cos\omega t & \cos(\omega t - \frac{2\pi}{3}) & \cos(\omega t + \frac{2\pi}{3}) \\ \frac{1}{2} & \frac{1}{2} & \frac{1}{2} \end{pmatrix} \begin{pmatrix} i_a \\ i_b \\ i_c \end{pmatrix} \quad (1)$$

If the phase A current is expressed by $i_a = I\sin\omega t - I_{off}$, then *dq* output currents can be rewritten by Eq. 1.

$$\begin{pmatrix} i_d \\ i_q \\ i_0 \end{pmatrix} = \begin{pmatrix} 1 & -\frac{2}{3}\sin\omega t \\ 0 & -\frac{2}{3}\cos\omega t \\ 0 & -\frac{1}{3} \end{pmatrix} \begin{pmatrix} I \\ I_{off} \end{pmatrix} \quad (2)$$

The *d*-axis and *q*-axis output currents become constant by current controller with the reference *dq* values with given value of current and 0, respectively. However, with space vector modulation, the zero-axis current remains unchanged and appears at the measured output current. Hence, the measured output current is obtained as Eq. 3

$$\begin{pmatrix} i_a \\ i_b \\ i_c \end{pmatrix} = \begin{pmatrix} \sin\omega t & \cos\omega t & 1 \\ \sin(\omega t - \frac{2\pi}{3}) & \cos(\omega t - \frac{2\pi}{3}) & 1 \\ \sin(\omega t + \frac{2\pi}{3}) & \cos(\omega t + \frac{2\pi}{3}) & 1 \end{pmatrix} \begin{pmatrix} I \\ 0 \\ -\frac{1}{3}I_{off} \end{pmatrix} \quad (3)$$

As shown in Eq.3, the offset current of any one phase results the offset currents of all three phases due to the current controller. Fig.2 shows the measured three-phase current, the measured *dq* current and the grid current when the offset I_{off} in phase A is changed from 0A to 9A at 0.3 s.

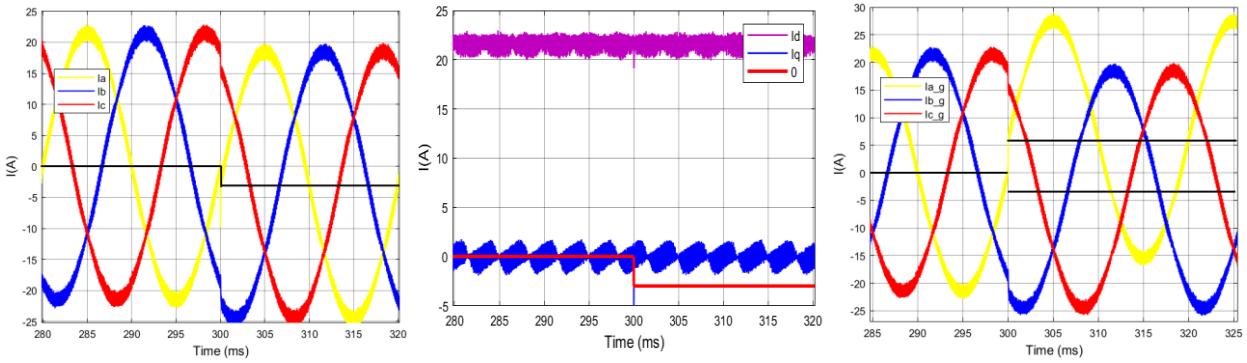

(a) (b) (c)

Fig. 2. Measured three-phase current (a), *dq* current (b) and grid current (c)

In Fig. 2(a), the measured three-phase current does not offset before 0.3s, but offsets down with the magnitude of -3A. Also, in Fig. 2(b), the zero-axis current does not offset before 0.3s, but offsets down with $I_0 = \frac{1}{3}I_{off} = -3\text{A}$. At this time, there is no offset in *dq* currents. In Fig. 2(c), the three-phase grid current does not offset before 0.3s, but the phase A grid current offsets up with the magnitude of 6A(=9A-3A), whereas the phase B and C grid currents offsets down with the magnitude of -3A. Comparing Fig. 2(a) and Fig. 2(c), only phase A current is different.

The following conclusions can be obtained from above analysis on the offset of the measured three-phase current.

First, the current offset cannot be accurately obtained by integrating each measured phase current because that it is difficult to find which phase current offset is occurred.

Second, if the grid current as well as the measure current is considered as shown from Fig. 2(a) and (c), the current offset can be obtained.

Third, assuming that a constant current is injected into the grid using only space vector modulation without current control, the current in the rotating reference frame oscillates with the grid frequency if there is an offset in the current detection. There is no offset in the grid current in practice. When the current controller is operated with constant d-axis and q-axis currents, the current offset happens the measured and grid currents. To overcome this problem, if the oscillating component of the grid frequency is added to the reference current, the offset of the grid current cannot be occurred.

Accordingly, the offset observer should be designed for accurate measuring of the current offset and the offset compensation method should be researched using the proposed offset observer.

III. Proposed current offset compensation method

A. Current offset observer design

Fig. 3 shows the structure of the proposed current-offset controller and the offset observer. Here, the *dq* reference currents are obtained from the active and reactive power reference values. The Current controller, inverter, filter and coordinate transformation are the same as the conventional system. [14] The inverter output voltage is expressed by

$$\begin{aligned} u_{inv\_a} &= r_a i_a + L_a \frac{di_a}{dt} - u_{g\_a} = r_a (i_{ac\_a} - i_{off\_a}) + L_a \frac{d(i_{ac\_a} - i_{off\_a})}{dt} + u_{g\_a} \\ u_{inv\_b} &= r_b i_b + L_b \frac{di_b}{dt} - u_{g\_b} = r_b (i_{ac\_b} - i_{off\_b}) + L_b \frac{d(i_{ac\_b} - i_{off\_b})}{dt} + u_{g\_b} \\ u_{inv\_a} &= r_a i_a + L_a \frac{di_a}{dt} - u_{g\_a} = r_a (i_{ac\_a} - i_{off\_a}) + L_a \frac{d(i_{ac\_a} - i_{off\_a})}{dt} + u_{g\_a} \end{aligned} \quad (4)$$

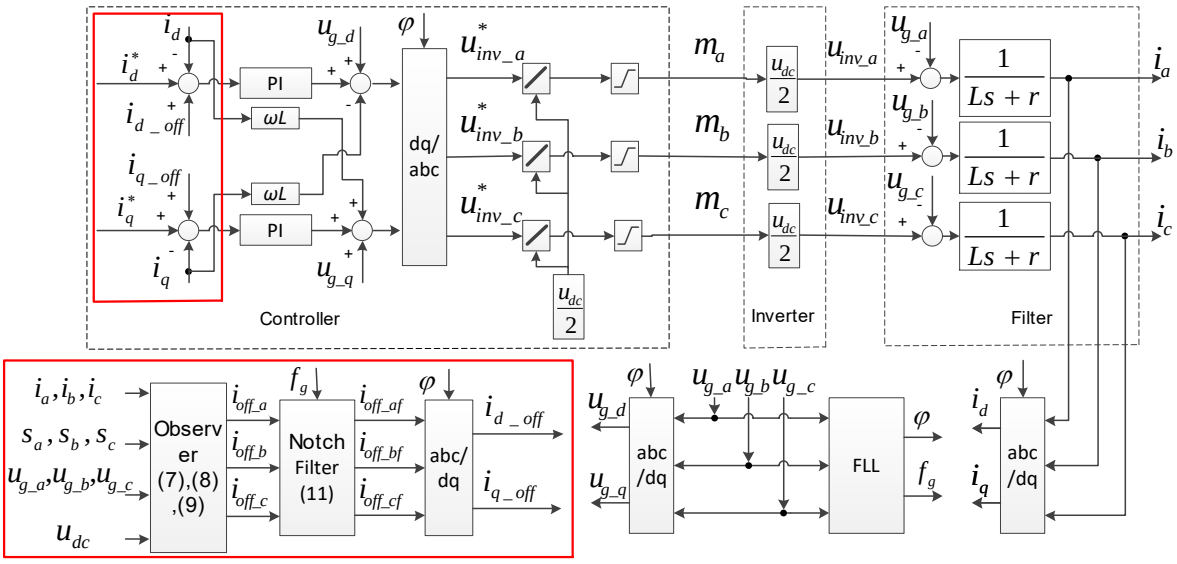

Fig. 3. Structure of the proposed current-offset controller and the offset observer

Where $r_a = r_b = r_c = r$, $L_a = L_b = L_c = L$

The Eq.4 can be simply rewritten as follows:

$$u_{inv\_x} = ri_x + L\frac{di_x}{dt} + u_{gx} = r(i_{ac\_x} - i_{off\_x}) + L\frac{d(i_{ac\_x} - i_{off\_x})}{dt} + u_{gx} \quad (5)$$

Where x means a, b and c.

The observer is usually given as follows in [24].

$$\begin{bmatrix} \dot{\hat{i}}_{off\_x} \\ \dot{\hat{i}}_{ac\_x} \end{bmatrix} = \begin{bmatrix} 0 & 0 \\ \frac{r}{L} & \frac{r}{L} \end{bmatrix} \begin{bmatrix} \hat{i}_{off\_x} \\ \hat{i}_{ac\_x} \end{bmatrix} + \begin{bmatrix} 0 \\ \frac{1}{L} \end{bmatrix} (u^*_{inv\_x} - u_{gx}) + \begin{bmatrix} k_1 \\ k_2 \end{bmatrix} \left[i_x - \hat{i}_x - \hat{i}_{off\_x} \right] \quad (6)$$

From Eq. 6, the current offset and the reference current are calculated as

$$\hat{i}_{off\_x} = \frac{k}{s+k}(i_x - \hat{i}_x) \quad (7)$$

$$\hat{i}_x = \frac{1}{Ls+r}(u^*_{inv\_x} - u_{gx}) \quad (8)$$

Where $\hat{i}_x$ is the output reference current of the inverter and $u^*_{inv\_x}$ is the output reference voltage of the inverter.

The reference current and the current offsets can be calculated from the Eq.7 and Eq.8.

B. Determination of the output reference voltage and current of the inverter

The inverter output reference voltage is needed not to measure but to calculate the inverter output terminal voltage. The output reference voltage of the inverter can be calculated based on the DC bus voltage and switching status of IGBTs.

$$\begin{aligned} u^*_{inv\_a} &= \frac{2S_a - (S_b + S_c)}{3} u_{dc} \\ u^*_{inv\_b} &= \frac{2S_b - (S_c + S_a)}{3} u_{dc} \\ u^*_{inv\_c} &= \frac{2S_c - (S_a + S_b)}{3} u_{dc} \end{aligned} \quad (9)$$

Where S_a, S_b, and S_c are the switching states of the upper arm IGBT, in which the state value is 1 when the switch turns on whereas the value is 0 when the switch turns off.

Then for the output reference current to track the grid current accurately, the inverter output reference current should be determined. If there is the DC offset, it is difficult to identify whether the grid current is biased. Therefore, the grid current value should be accurately obtained regardless of the measurement of the offset current or the operation of the offset controller.

The inverter output reference current is simply calculated by the Eq. 8 in which the inverter output reference voltage and the grid voltage are used. The current obtained from the Eq. 8 tracks the grid current.

As can be seen from Eq. 8, the inverter output reference current is related to the inductance and resistance of the filter as a first order inertial segment. Accordingly, the filter design method should be explained in detail in the offset current controller design. Output reference voltages may get by using voltage sensing circuit[8, 9].

C. Current offset calculation

The current offset value is calculated with the measured current and the output reference current by Eq. 7. Once the current offset is obtained, the compensation value is calculated using the Clarke and Park transformation and is reflected in the *dq* reference current to compensate the current offset.

- Filter Design

According to Eq. 7, the low-pass filter is used to calculate the current offset by using the error between the grid current and the reference current. The cutoff frequency of the low-pass filter is set to 5 Hz for the design of filter and then the transfer function of the filter is

$$G_f(s) = \frac{k}{s+k} \tag{10}$$

Where k is the coefficient of filter

- Notch Filter Design

The output current of the observer includes the current component oscillating with the supply frequency. If the output filter parameters are varied, the current is more largely oscillated. This oscillation can be eliminated using a Notch filter. On other words, because the supply frequency is fluctuated continuously, the cutoff frequency of this filter should be tracked the supply frequency. The transfer function of the Notch filter is

$$F(s) = \frac{s^2+\omega_g^2}{(s+\omega_g)^2} = \frac{s^2+4\pi^2 f_g^2}{(s+2\pi f_g)^2} \tag{11}$$

The discretization of the filter using bilinear transformation yields

$$F(z) = \frac{b_0 + b_1 z^{-1} + b_2 z^{-2}}{1 + a_1 z^{-1} + a_2 z^{-2}} \tag{12}$$

Where

$$a_1 = \frac{2T_s^2 f_g^2 \pi^2 - 2}{a} \qquad a_2 = \frac{T_s^2 f_g^2 \pi^2 - 2T_s f_g \pi + 1}{a}$$

$$a = T_s^2 f_g^2 \pi^2 + 2T_s f_g \pi + 1$$

$$b_0 = \frac{T_s^2 f_g^2 \pi^2 + 1}{a} \qquad b_1 = \frac{2T_s^2 f_g^2 \pi^2 - 2}{a} \qquad b_2 = \frac{T_s^2 f_g^2 \pi^2 + 1}{a}$$

where f_g is the supply frequency, T_s is the sampling period.

D. Current offset controller design

The offset of output current can be eliminated by directly adding the current offset obtained from the observer to the current detection loop. However, it is noted that the offset of output current cannot be eliminated completely by above-mentioned direct current-offset compensation method due to the variation of the offset current.

Therefore to overcome this problem, the *dq* components of offset current should be added to the current reference of the current controller but to the current detection loop. This allows the current controller to be used as a current offset controller without the additional design of the current offset controller. The current controller is designed as a PI controller where the proportional and integral coefficients are calculated by

$$\frac{k_i}{k_p} = \frac{r}{L} \ , \ \frac{k_p}{L} = \frac{1}{\tau} \qquad (13)$$

where k_p and k_i are proportional and integral coefficients, respectively, r and L are the resistyance and inductance of the filter, respectively, τ is the time constant of the closed-loop system.

Also, the plant transfer function is given by

$$G(s) = \frac{1}{Ls + r} \qquad (14)$$

IV. Simulation result

The characteristics of the proposed method are analyzed through MATLAB Simulink. Fig. 4 shows the power plant configuration and Fig. 5 shows the proposed observer and current controller. The parameters of the plant and the current-offset controller designed by the proposed method are given in Table 1.

The phase, the voltage and current at the *dq* rotating reference frame were calculated from the grid voltage and current. For the simulation, the phase current is obtained by adding the virtual offset value to the grid current. Also the inverter output voltage reference is obtained through Eq. 9, the output current reference and the current offset are determined from Eq. 8 and Eq. 7, respectively.

Then, the Notch filter is used to obtain the accurate current offset with the elimination of the ripple component. For the simulation, the d-axis component of the output current is gradually increased from zero to rated current but the q-axis current component is set to zero. The current controller is constructed as shown in controller block diagram of Fig. 3.

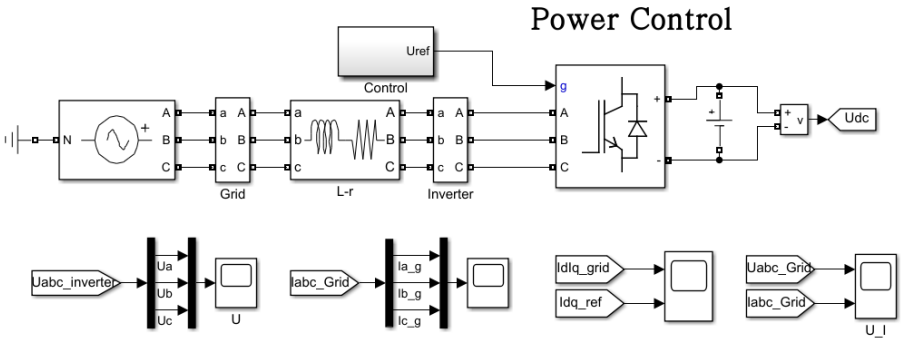

Fig. 4. Power Plant Configuration in Matlab

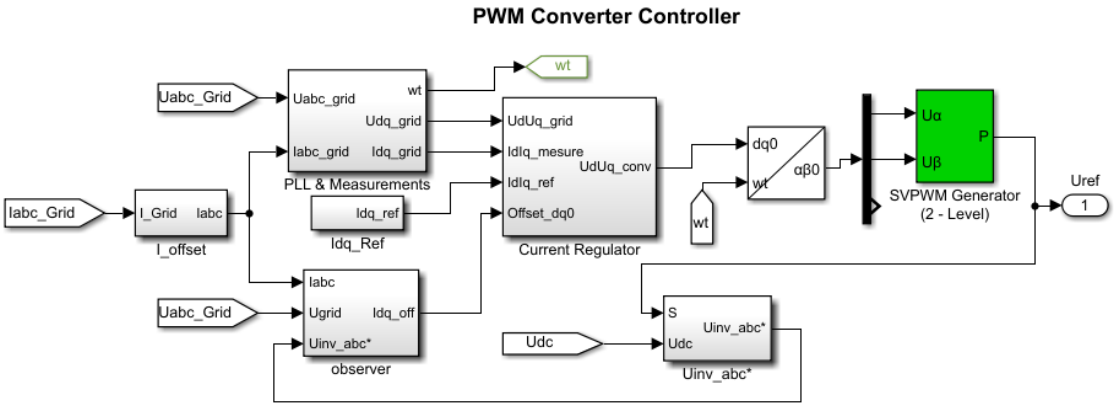

Fig. 5. Structure of the proposed controller and observer.

Table. 1. Parameters of the plant and controller in simulation.

Parameter	Value	Parameter	Value
P	10kW	τ	250μs
L	2mH	f_{samp}	20kHz
r	1mΩ	f_{pwm}	10kHz
U_{dc}	680V	k_p	8
f_g	50Hz	k_i	4
U_g	380V	k	31.4

A. Inverter output reference voltage

The inverter output voltage and output reference voltage are shown in the Fig. 6. As can be seen from Fig. 6, the inverter output voltage reference is approximated with the actual inverter output voltage according to the inverter output reference voltage calculated by Eq. 9. The inverter output voltage and the output reference voltage are shown in the enlarged waveforms of Fig. 6. The inverter output reference voltage tracks accurately the inverter output voltage even if the current is offset or the offset controller is operated.

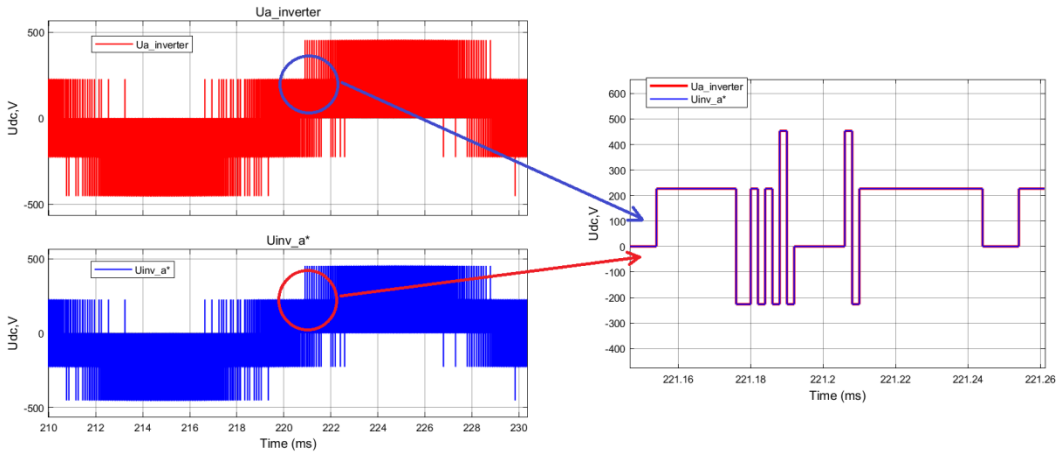

Fig. 6. Inverter output voltage and output reference voltage waveform

B. Inverter output reference current

Fig.7 shows the grid current, the inverter output reference current and the measured current waveforms. At t=0.3 s, the phase A current is offset to 9A, and at t=0.4 s the offset controller is operated to compensate the offset of the grid current. As shown in Fig. 7a, the grid current is asymmetryed at t=0.3 s and in detail, the phase A is offset up to 6 A, but the phase B and C are offset down to 3 A. At t=0.4 s, the current offset controller is operated so that the grid current is kept to symmetry current again. As shown in Fig. 7b, the inverter output reference current is changed to approximate with the grid current.

The measured current waveform is shown in Fig. 7c. When the current offset is occurred at 0.3s, the three-phase current is adjusted by the current controller and the measured currents of phase A, B and C are offset down to 3A. That is, by the measured current waveform, the phase occuring current offset can not be found. With the current offset controller operating at 0.4 s, the phase B and phase C currents are changed symmetrically, and only phase A current is offset down to 6 A.

Fig. 7d shows the grid current, inverter output reference current and measured current waveforms of phase A before the offset current is occurred at t=0.25 s. As can be seen, all three currents are identical. Fig. 7e shows the grid current, inverter output reference current and measured current waveform of phase A when the offset current is occurred at t=0.38s. As can be seen, the offset current is occurred, the measured current is offset down to 3A, while the grid current and inverter output reference current are offset up to 6A. The inverter output reference current tracks accurately the grid current even in the presence of current pffset. Fig. 7f shows the grid current, reference current and measured current waveforms of phase A when the current offset controller is operated at t=0.45s. the current offset does not be existed in the grid current and reference current , and in the measured current is offset down to 9 A. In this case, the reference current is accurately estimated by the grid current.

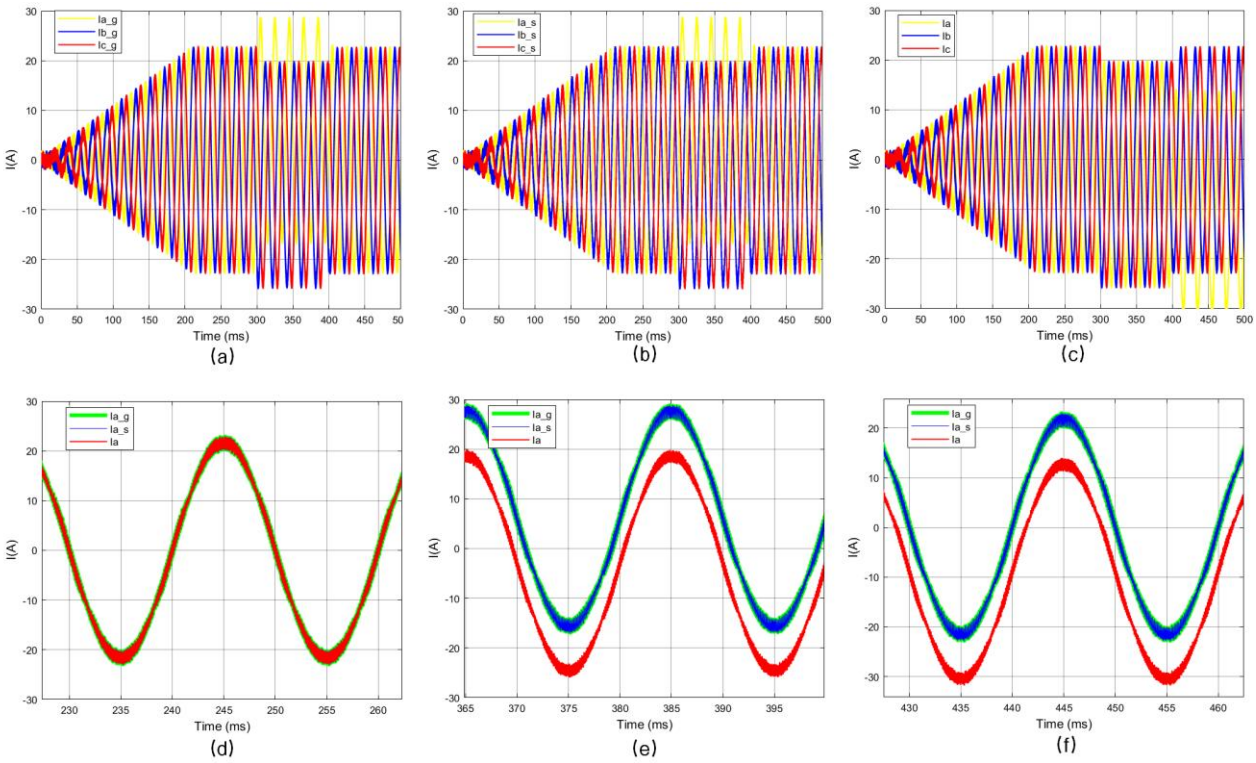

Fig. 7. Grid current, inverter output reference current and measured current waveform

(a) Grid current waveform (b) Inverter output reference current waveform, (c) Measured current waveform, (d) Three types of current waveform in normal state(0.25s), (e) Three types of current waveform in offset state (0.38s), (f) Three types of current waveform in offset control state (0.45s).

C. Current offset calculation

Case 1: *Current offset of three phase*

Fig. 8 shows the characteristic waveforms for three phase when the currents of phase A, B and C are offset as 9A, -3A and 6A at *t*=0.3s, respectively. As shown in Fig. 8a, when the offset currents are occurred in phase A, B and C at *t*=0.3s, the offset currents of the phase A , B and C are exactly observed as 9A, -3A and 6A by the proposed observer, respectively. Fig. 8b, Fig. 8c and Fig. 8d show that by the proposed observer, the current offset of phase A, B and C are observed as zero initially before *t*=0.3s, but the offset currents of phase A, B and C are observed as 9 A, -3 A and 6A after *t*=0.3 s, respectively.

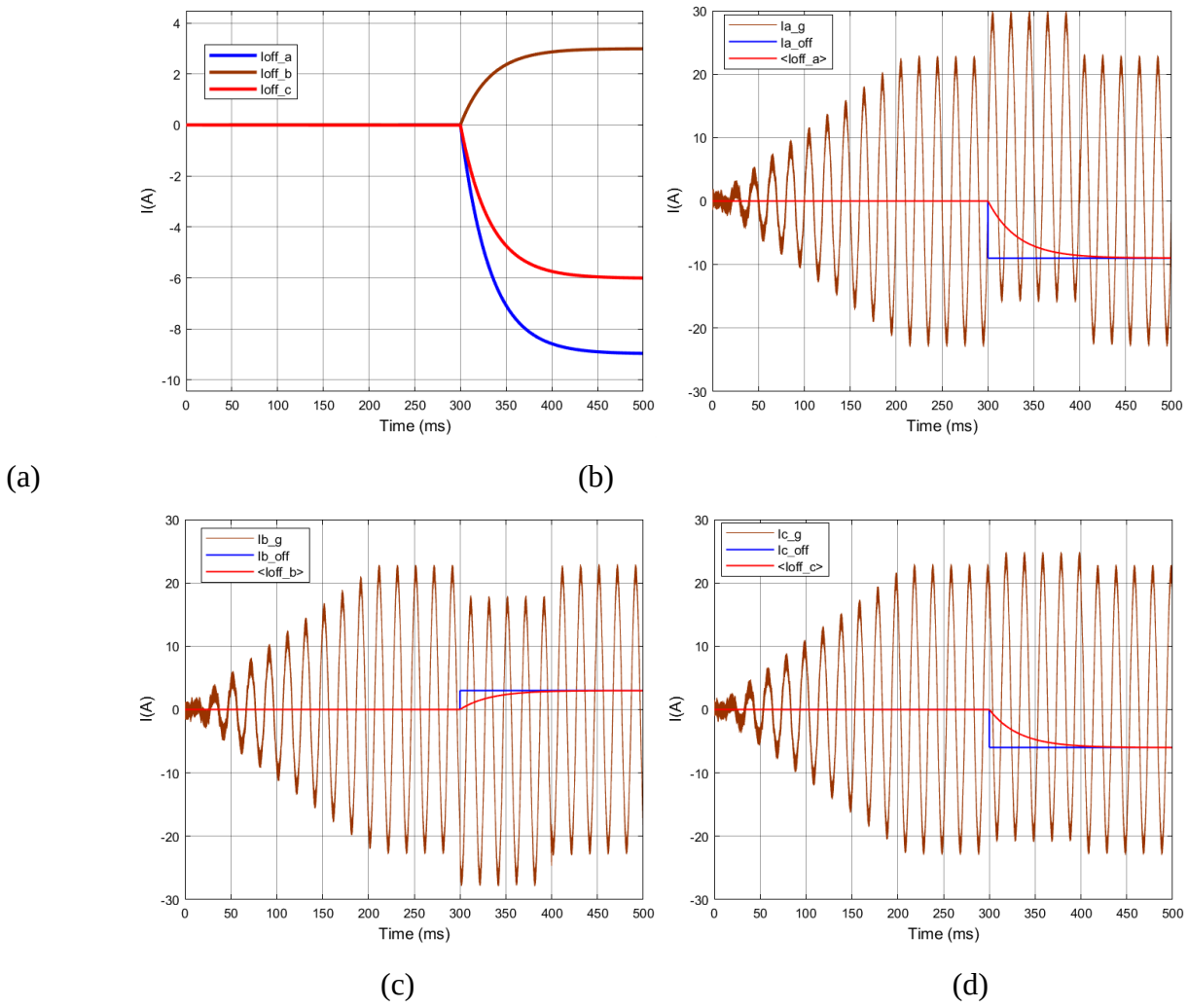

Fig. 8. Observed offset current, Phase A currents, Phase B currents and Phase C current

(a) Thee phase observed offset currents, (b) Grid current, offset value and observed offset current in Phase A, (c) Grid current, offset value and observed offset current in Phase B, (d) Grid current, offset value and observed offset current in Phase C

Case* 2: *Variation of filter parameters

Here, the compensation of the current offset by the proposed current offset compensation method is analysed when the filter parameters are varied.

Initially, it is supposed that the parameters of the controller and digital filter are unchanged but the output filter parameters are given to R=0.5mΩ, L=1mH unlike of R=1mΩ, L=2mH.

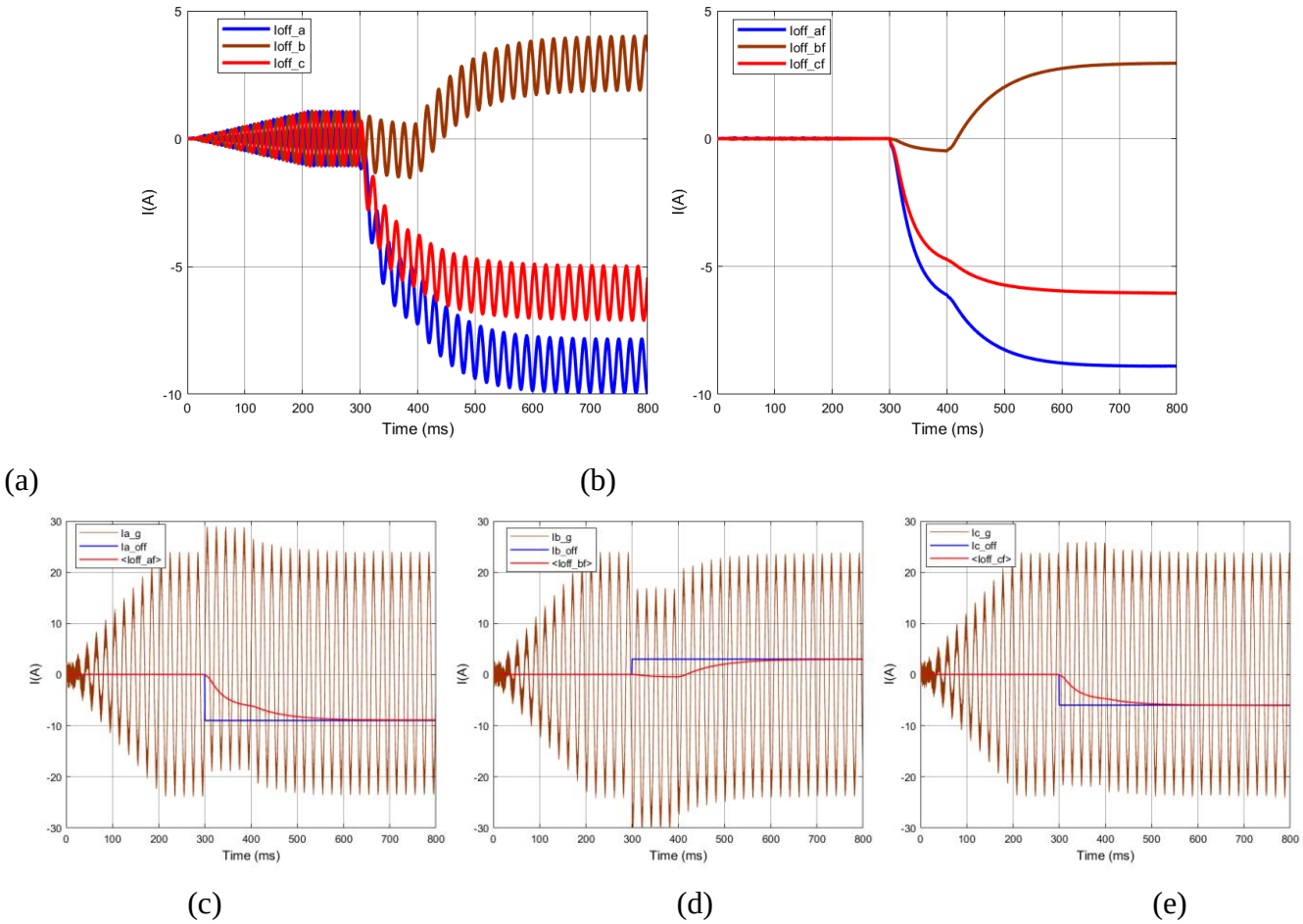

Fig. 9. Observed offset current, Phase A currents, Phase B currents and Phase C current

(a) Thee phase observed offset currents, (b) Three phase offset currents after Notch filtering, (c) Grid current, offset value and observed offset current in Phase A, (d) Grid current, offset value and observed offset current in Phase B, (e) Grid current, offset value and observed offset current in Phase C

Because output reference current is changed by Eq. 8 due to the variation of the filter parameters, the output of the current-offset observer ripples with the supply frequency as shown in Fig 9a. To remove the ripple component, the notch filter is applied in this paper. Fig 9b shows that the output of the current-offset observer which is filtered by the notch filter tracks the current offset.

Fig 9c, 9d and 11e show that in the phase A, B and C, the observed offset currents do not track the current offset only by the current-offset observer before t=0.4s, but the observed offset currents begin to track the current offset by both the current-offset observer and the current–offset controller after t=0.4s and accurately track the current offset after t=0.5s.

D. Current offset controller

The reference current of the current-offset controller and the output current waveforms in *dq* rotating frame are shown in Fig 10. As shown in the Fig 10, the reference current is constant before the current-offset controller is operated, but the reference current is rippled with the supply frequency after the current-offset controller is operated. At this time, the current -offset controller accurately tracks the reference current to compensate the current offset.

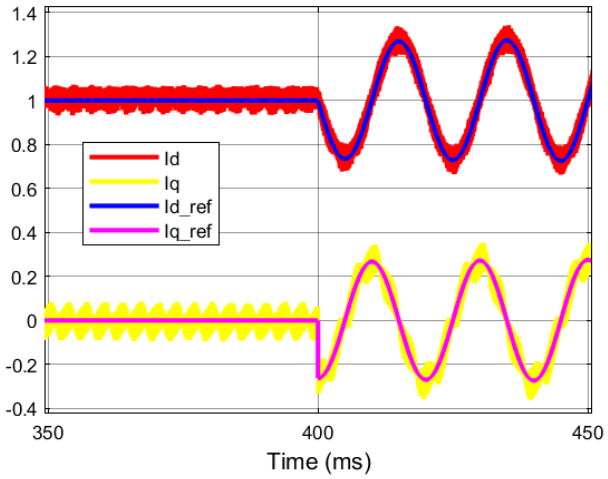

Fig. 10. Reference current of the current-offset controller and output current waveforms in *dq* rotating frame

V. Conclusion

In this paper, the current-offset compensation method for three-phase grid-connected inverter without output transformer has been investigated. In the proposed method, the current offset and the reference current are calculated using the current-offset observer and the current offset is compensated using a PI controller. Even if the filter parameters are changed, the proposed method can observe the current offset accurately and the current offset controller accurately compensates the current offset. The application of the observer and controller designed in this paper effectively compensates the three-phase current offset. The proposed method can also be used in current control of motor drive systems in rotating frame.

REFERENCES

[1] J. M. Carrasco, L. G. Franquelo, J. T. Bialasiewicz, E. Galvan, R. C. Portillo Guisado, M. A. M Prats, J. I. Leon, and N. Moreno-Alfonso, "Power-electronic systems for the grid integration of renewable energy sources: A survey" IEEE Trans. Ind. Electron., vol. 53, no. 4, pp. 1002–1016, Jun. 2006.

[2] D. G. Infield, P. Onions, A. D. Simmons, and G. A. Smith, "Power quality from multiple grid-connected single-phase inverters," IEEE Trans. Power Del., vol. 19, no. 4, pp. 1983–1989, Oct. 2004

[3] S. B. Kjaer, J. K. Pedersen, and F. Blaabjerg, "A review of single-phase grid-connected inverters for photovoltaic modules," IEEE Trans. Ind. Appl., vol. 41, no. 5, pp. 1292–1306, Sep. 2005.

[4] W. M. Blewitt, D. J. Atkinson, J. Kelly, and R. A. Lakin, "Approach to low-cost prevention of DC injection in transformerless grid connected inverters," IET Power Electron., vol. 3, no. 1, pp. 111–119, Jan. 2010.

[5] G. Buticchi, E. Lorenzani, and G. Franceschini, "A DC offset current compensation strategy in transformerless grid-connected power converters" IEEE Trans. Power Del., vol. 26, no. 4, pp. 2743–2751, Oct. 2011.

[6] M. Armstrong, D. J. Atkinson, C. M. Johnson, and T. D. Abeyasekera,"Auto-calibrating DC link current sensing technique for transformerless, grid connected, H-Bridge inverter systems," IEEE Trans. Power Electron.,vol. 21, no. 5, pp. 1385–1393, Sep. 2006.

[7] L. Bowtell and A. Ahfock, "Direct current offset controller for transformerless single-phase photovoltaic grid-connected inverters," IET Renew. Power Gener., vol. 4, no. 5, pp. 428–437, Sep. 2010.

[8] G. He, M. Chen, N. Su, R. Xie, and D. Xu, "A novel control strategy to suppress DC current injection of single-phase PV inverter to the grid," presented at the IEEE Power Electronics for

Distributed Generation Systems Conference, Rogers, AR, USA, Jul. 8–11, 2013.

[9] G. He, D. Xu, M. Chen "A Novel Control Strategy of Suppressing DC Current Injection to the Grid for Single-Phase PV Inverter" IEEE Trans. Power Electron., vol. 30, no. 3, pp. 1266–1274, Mar. 2015.

[10] R. Gonzalez, J. L ´ opez, P. Sanchis, and L. Marroyo, "Transformerless inverter for single-phase photovoltaic systems," IEEE Trans. Power Electron., vol. 22, no. 2, pp. 693–697, Mar. 2007.

[11] Y. Cho, "Observer based online current offset compensation method for single-phase photovoltaic inverter applications" IEEE ELECTRONICS LETTERS, vol. 48, no. 23, Nov. 2012.

[12] X. Guo, W. Wu, W. Herong, and G. San, "DC injection control for grid connected inverters based on virtual capacitor concept," in Proc. IEEE Elect. Mach. Syst. Conf., Wuhan, China, Oct. 17–20, 2008, pp. 2327–2330.

[13] Q. Yan, X. Wu, X. Yuan, Y. Geng and Q. Zhang, "Minimization of the DC Component in Transformerless Three-Phase Grid-Connected Photovoltaic Inverters" IEEE Trans. Power. Electron., vol. 30, no. 7, pp. 3984–3997, July. 2015

[14] A. Yazdani , R. Irava, "Voltage-Sourced Converters in Power Systems" JOHN WILEY & SONS, pp. 204–224, 2010

[15] Md. Ashib Rahman, Md. Rabiul Islam, A. M. Mahfuz-Ur-Rahman, Kashem M. Muttaqi, and Danny Sutanto, "Investigation of the Effects of DC Current Injected by Transformer-Less PV Inverters on Distribution Transformers" IEEE Trans. Appl. Supercond., vol. 29, no. 2, Mar. 2019, Art. no. 0602904

[16] B. Guo et al., "Cost-Effective DC Current Suppression for Single-Phase Grid-Connected PV Inverter," in IEEE J. Emerg. Sel. Topics Power Electron., Oct. 2020.

[17] Q. N. Trinh, P. Wang, Y. Tang, L. H. Koh and F. H. Choo, "Compensation of DC Offset and Scaling Errors in Voltage and Current Measurements of Three-Phase AC/DC Converters," in IEEE Trans. Power Electron., vol. 33, no. 6, pp. 5401-5414, June 2018

[18] W. Zhang, M. Armstrong and M. A. Elgendy, "Mitigation of DC Current Injection in Transformer-Less Grid-Connected Inverters Using a Voltage Filtering DC Extraction Approach," in IEEE Trans. on Energy Convers., vol. 34, no. 1, pp. 426-434, March 2019

[19] B. Long, L. Huang, and H. Sun, "An intelligent dc current minimization method for transformerless grid connected photovoltaic inverters," in Int. Soc. Autom., vol. 88, pp. 268–279, 2018.

[20] W. Zhang, M. Armstrong and M. A. Elgendy, "DC Injection Suppression in Transformer-Less Grid-Connected Inverter using a DCLink Current Sensing and Active Control Approach," in IEEE Trans. Energy Conver., vol. 34, no. 1, pp. 396-404, March 2019.

[21] A. Abdelhakim, P. Mattavelli, D. Yang and F. Blaabjerg, "Coupled Inductor-Based DC Current Measurement Technique for Transformerless Grid-Tied Inverters," in IEEE Trans. Power Electron., vol. 33, no. 1, pp. 18-23, Jan. 2018

[22] H. Xiao, "Overview of Transformerless Photovoltaic Grid-Connected Inverters," in IEEE Trans. Power Electron., vol. 36, no. 1, pp. 533-548, Jan. 2021.

[23] Z. Shi, B. Wu, J. Liao, G. Qiu,, "Suppressing DC Current Injection in Transformerless Grid-Connected Inverter Using A Customized Current Sensor," IEEE POWER ELECTRONICS REGULAR PAPER., May 2021

Kwakernaak, Huibert "LINEAR OPTIMAL CONTROL SYSTEMS" WILEY 1972